Anomalous vortex dynamics in the spin-triplet superconductor UTe_2

Y. Tokiwa,[1,*] H. Sakai,[1] S. Kambe,[1] P. Opletal,[1] E. Yamamoto,[1] M. Kimata,[2] S. Awaji,[2] T. Sasaki,[2] Y. Yanase,[3] Y. Haga,[1] and Y. Tokunaga[1]

[1]*Advanced Science Research Center, Japan Atomic Energy Agency, Tokai, Ibaraki 319-1195, Japan*

[2]*Institute for Materials Research, Tohoku University, Sendai 980-8577, Japan*

[3]*Department of Physics, Kyoto University, Kyoto 606-8502, Japan*

(Received 15 May 2023; revised 20 July 2023; accepted 13 September 2023; published 4 October 2023)

The vortex dynamics in the spin-triplet superconductor UTe_2 are studied by measuring the dc electrical resistivity with currents along the a axis under magnetic fields along the b axis. Surprisingly, we have discovered an island region of low critical current deep inside the superconducting (SC) state, well below the SC upper critical field, attributed to a weakening of vortex pinning. Notably, this region coincides with the recently proposed intermediate-field SC state. We discuss the possibility of nonsingular vortices in the intermediate state, where the SC order parameter does not vanish entirely in the vortex cores due to the mixing of multiple SC components.

DOI: 10.1103/PhysRevB.108.144502

I. INTRODUCTION

Unconventional superconductivity often leads to unconventional vortex states. In conventional cases, the thermodynamic superconducting (SC) transition and the formation of a vortex lattice occur simultaneously at T_c. However, in unconventional superconductors, these could appear sequentially due to their anomalously large T_c compared with their condensation energy per coherent volume, leading to the formation of a vortex liquid state in a region below T_c [1]. Since the lattice constant of the vortex continuously decreases with increasing magnetic field, a vortex lattice melts above a magnetic field close to B_{c2}, when the amplitude of vortex lattice fluctuations becomes comparable to the lattice constant [1].

Among heavy fermion compounds, URu_2Si_2 and UCoGe exhibit unusually wide regions of vortex liquid states [2,3]. For URu_2Si_2, the capability of growing ultraclean crystals clearly contributed to the observation of a liquid state [2]. The situation is more complex for UCoGe, since the compound exhibits spin-triplet SC and the vortex liquid state is accompanied by a field reinforcement of superconductivity for the field applied along a magnetically hard axis [3]. There, the weakening of the pinning force due to the formation of nonsingular fractional vortices has been discussed [3]. Such fractional vortices may host Majorana fermions, which obey non-Abelian statistics [4,5]. These studies stimulate our interest in investigating the vortex dynamics in the spin-triplet superconductor UTe_2 [6–17], which was recently shown to have multiple SC states under magnetic fields along the magnetic hard b axis [9,10,12,14,18].

For UTe_2, significant efforts have been made to improve crystal quality [19–21]. The recent progress of growing clean crystals has led to the observation of quantum oscillations [21–25] and renewed the SC phase diagram with higher B_{c2} [18,26]. The reinforcement of superconductivity occurs for the field along the b axis, where the applied field initially suppresses superconductivity, but enhances T_c above $B^\star \sim 15$ T, causing a minimum of $T_c(B)$ at $B^\star$ [6,8,12]. The recent studies have revealed the presence of a phase boundary within the SC state for $B \| b$, which divides the superconductivity into low- and high-field SC states [10,12]. Most recently, another phase boundary has been found in the low-field SC state around $B^\star$, implying the presence of, in total, three SC states with the intermediate-field SC (IFSC) state, which may be characterized by a mixture of multiple SC order parameters from the low- and high-field SC states (LFSC and HFSC states) [18,27].

In this paper, using an ultraclean single crystal grown using the molten-salt flux method [21], we study the vortex dynamics in the multiple SC states of UTe_2. Remarkably, our direct current (dc) electrical resistivity measurements with different currents reveal a sudden weakening of the pinning force in the IFSC state for $B \| b$ [18]. This may be caused by the formation of nonsingular vortices in the IFSC state, where the SC order parameter does not vanish entirely in vortex cores due to the mixing of multiple SC components.

II. EXPERIMENTAL

The dc resistivity measurements were performed using the four-probe method and a ^{3}He cryostat with an SC magnet at the High-Field Laboratory for Superconducting Materials at the Institute for Materials Research at Tohoku University. The sample was placed inside ^{3}He liquid during the measurements. The rod-shaped sample used for the measurements has a cross-sectional area of $0.29 \times 0.26 = 0.075$ mm^2 and a length of 2.2 mm along the a axis between the voltage contacts. Magnetic field was applied along the b axis. The sample, grown using the molten-salt flux method, has a SC transition

*ytokiwa@gmail.com

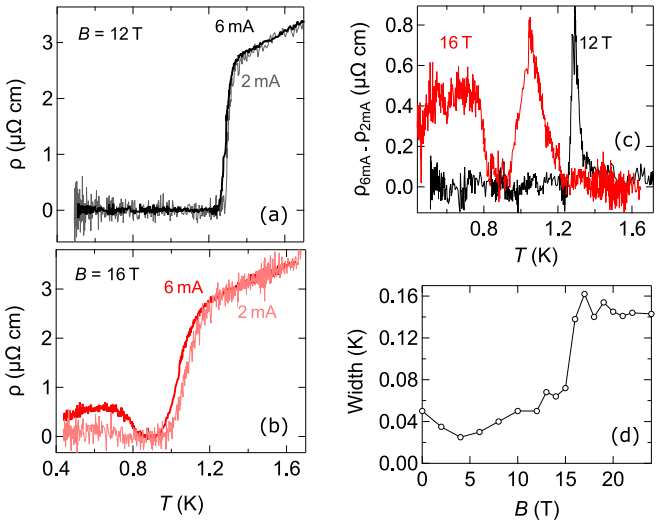

FIG. 1. The dc resistivity of UTe_2 measured with different currents, 2 mA (gray, pink) and 6 mA (black, red) along the a axis under magnetic fields of 12 T (a) and 16 T (b) along the b axis. (c) The difference between the resistivity with the two currents, $\rho_{6\mathrm{mA}} - \rho_{2\mathrm{mA}}$, at $B = 12$ and 16 T. (d) Magnetic field dependence of the full width of half maximum for the peak observed in $\rho_{6\mathrm{mA}} - \rho_{2\mathrm{mA}}$ at the normal-conducting–superconducting transition temperature.

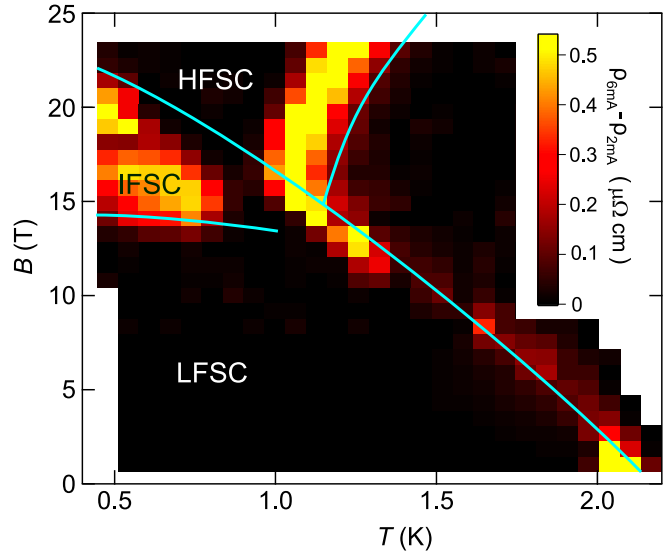

FIG. 2. Color contour plot of the difference $\rho_{6\mathrm{mA}} - \rho_{2\mathrm{mA}}$. The plot is constructed from the temperature-dependent dc resistivity $\rho(T)$ measurements at various magnetic fields. Values of $\rho(T)$ at 2 and 6 mA are taken at magnetic fields from 0 to 12 T with an interval of $\Delta B = 2$ T, taken from 13 to 22 T with $\Delta B = 1$ T, and taken finally at 24 T. The solid blue lines are the phase boundaries determined by the recent study [21]. LFSC, IFSC, and HFSC, low-field, intermediate-field, and high-field superconducting states, respectively [21].

temperature of $T_c = 2.1$ K [21]. The Joule heating effect was examined by applying current in the normal conducting state at a temperature of 1.46 K and in magnetic field of 20 T. The voltage shows no deviation from the linear dependence of the electrical current I within the experimental accuracy up to 60 mA. Above this current, it deviates with an upward curvature due to heating. We can neglect the Joule heating effect because the upper bound of the Ohmic region, 60 mA, is 10 times larger than the typical current, 6 mA, and larger than the maximum current of 45 mA for measurements of E-J characteristics.

III. RESULTS

Figures 1(a) and 1(b) show the dc resistivity with two different currents, 2 and 6 mA, along the a axis under magnetic fields of 12 and 16 T along the b axis. While the SC transition is sharp at $B = 12$ T, it broadens significantly at 16 T. The data with 6 mA at 16 T show zero resistance below 1 K and remarkably recover nonzero resistance below 0.8 K. The difference between ρ measured by the two different currents, $\rho_{6\mathrm{mA}} - \rho_{2\mathrm{mA}}$, is plotted in Fig. 1(c). A peak at the normal-conducting–superconducting (NC-SC) transition temperature, T_c, is clearly broader for $B = 16$ T than for $B = 12$ T. The full width at half maximum of the peak at T_c is plotted in Fig. 1(d). The position of stepwise increase, $B = 15$ T, coincides with the multicritical point of different SC states, $B^\star$ [10,12,18]. This result is consistent with the reported broadening of the transition for the high-field reinforced SC state [12,18].

From resistivity measurements at various magnetic fields, we constructed the color contour plot of $\rho_{6\mathrm{mA}} - \rho_{2\mathrm{mA}}$ as shown in Fig. 2. It reproduces the peculiar NC-SC phase boundary with the reinforcement of superconductivity above $B^\star \sim 15$ T. Our $T_c(B)$ values agree well with the reported ones for low fields below $B^\star$, whereas they are slightly shifted to lower temperatures by ~0.2 K at high fields above $B^\star$. The shift only for the HFSC state is explained by a sample misalignment of ~2° from $B \parallel b$ axis, because T_c for the HFSC state is very sensitive to the field angle, whereas that for the LFSC state is much less sensitive [18].

The peculiar behavior of $\rho(T)$ with 6 mA at $B = 16$ T indicates that the vortices form a solid below T_c and start to flow below 0.8 K. For 2 mA, vortices remain solid down to 0.45 K. The vortex-flow state for 6 mA corresponds to the finite $\rho_{6\mathrm{mA}} - \rho_{2\mathrm{mA}}$ region deep inside the SC state, which spans magnetic fields of 14–21 T and temperatures below 0.8 K. Here, it should be mentioned that the color coding in Fig. 2 does not represent the vortex-flow resistivity, $\rho_f = dE/dj$, where E and j are the electric field and current density, respectively. It rather highlights the region of low critical current because the light color indicates the region of critical current lower than 6 mA. More detailed investigations of the vortex-flow resistivity are left for future studies. It is also important to note that $\rho_{2\mathrm{mA}} = 0$ throughout the entire SC state, including the IFSC state, with the exception of the region directly below T_c. This observation indicates finite j_c, except for the region immediately below T_c.

As shown in Fig. 1(c), $\rho_{6\mathrm{mA}} - \rho_{2\mathrm{mA}}$ at 16 T exhibits the two vortex-flow states right below T_c and below 0.8 K, separated by a solid state around 0.9 K. Such a separation is always observed in any magnetic fields of our $\rho(T)$ measurements between 12 and 22 T, with an interval of 1 T. Because thermal fluctuations increase with temperature, fluctuation-induced vortex flow would not disappear with increasing temperature but rather persists up to T_c. Therefore the formation of the

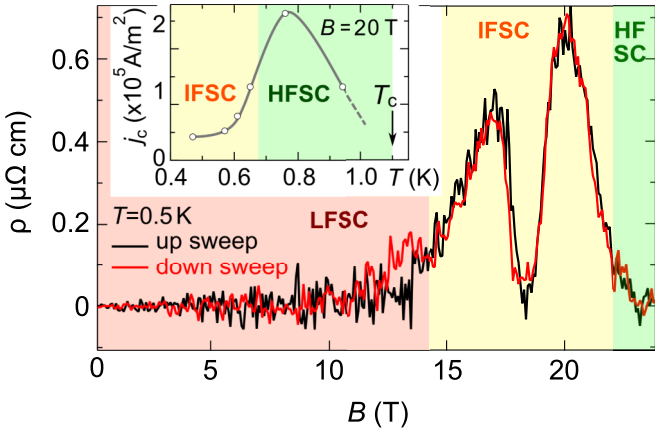

FIG. 3. Magnetic field dependence of the resistivity of UTe_2 at a temperature of 0.5 K for the field along the b axis with a current of 6 mA along the a axis. The black and red curves are the data taken by sweeping the magnetic field up and down, respectively. The red, yellow, and green colored regions labeled as LFSC, IFSC, and HFSC are the low-field, intermediate-field, and high-field superconducting states, respectively. The inset shows the critical current density, j_c, at $B = 20$ T which is needed to induce finite resistivity. "T_c" denotes the normal-conducting–superconducting phase transition determined by zero resistance with a small current of 0.5 mA.

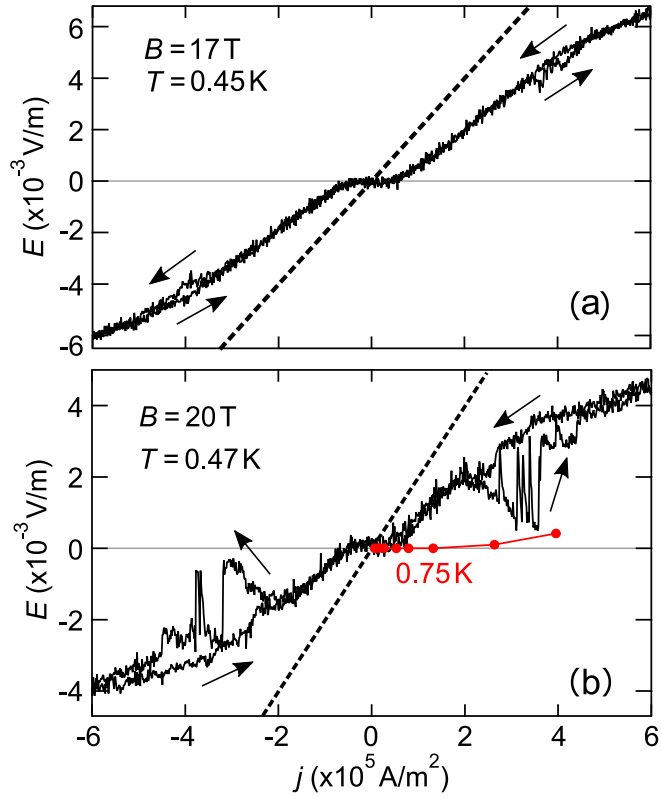

FIG. 4. Electric-field–current (E-J) characteristics deep inside the SC state at $B = 20$ and 17 T. Dashed lines represent the resistivity of the NC state, which is determined by extrapolating the NC resistivity with T^2 dependence to the measurement temperatures for E-J characteristics. Data at $T = 0.75$ K for $B = 20$ T are plotted for comparison (red). The maximum current density corresponds to a current of 45 mA.

island region of low critical current deep inside the SC state is ascribed to weakening of vortex pinning. Reflecting the separation, the critical current density j_c, needed to induce finite resistivity, exhibits an unusual maximum as a function of temperature and decreases on entering the IFSC state (inset of Fig. 3).

Notably, there is a narrow field range around 18 T of $\rho_{6\mathrm{mA}} - \rho_{2\mathrm{mA}} = 0$ in the middle of the low-j_c region. This separates the low-j_c region into lower- and higher-field ones, spanning 14–17 and 19–21 T, respectively. This is not an experimental error but rather reproducible. The magnetic field dependence of $\rho_{6\mathrm{mA}}$ clearly indicates vortex solidification with $\rho_{6\mathrm{mA}} = 0$ at 18 T between the two flow states with nonzero $\rho_{6\mathrm{mA}}$ (Fig. 3). There is no clear hysteresis between the data for sweeping magnetic field up and down. The field range of solidification is independent of temperature. Therefore it might be caused by a kind of matching effect of vortices.

Figures 4(c) and 4(d) show the E-j characteristics in the two regions of low j_c. They indicate a narrow $E = 0$ region of the vortex solid state for $|j| < 4 \times 10^4$ A/m^2 (3 mA). On the other hand, at an elevated temperature of 0.75 K for $B = 20$ T, the critical current density 27×10^4 A/m^2 to induce nonzero E is much larger. Interestingly, both data sets at 17 and 20 T display unusual current-density dependence. At 20 T, E increases with j in the low-j region, but it turns to decreasing above $j = 2 \times 10^5$ A/m^2 and almost reaches $E = 0$ (solidification). Furthermore, we note that E shows repeated sharp changes between the low and high values in the j range. This indicates that less-movable vortices suddenly flow at random j values, released from vortex pinning. This behavior is reproducible in the reversed current direction ($j < 0$) and occurs only for sweeping up the magnitude of the current density $|j|$, resulting in the hysteresis. At 17 T, the same but much weakened behavior is observed at a slightly elevated $|j|$ range. Additionally, the slope becomes smaller in the same $|j|$ range. The origin of the stronger pinning force in this $|j|$ range calls for future studies.

IV. DISCUSSION

We discuss the possible origins of the weakening of the pinning force deep inside the SC state. The vortex-flow region shown in Fig. 2 coincides well with the recently proposed IFSC state, which has a lower-field phase boundary around 14 T [18]. Therefore the weaker pinning force arises from the properties of the IFSC state [18,27].

With the orthorhombic crystal structure of UTe_2, the SC states are classified into $A_u^{\|b}$ or $B_u^{\|b}$ irreducible representations when the magnetic field is applied along the b axis [27]. Using the classification of the odd-parity SC order parameters for the point group D_{2h} at zero field, the $A_u^{\|b}$ and $B_u^{\|b}$ states are represented as $A_u^{\|b} = A_u + B_{2u}$ and $B_u^{\|b} = B_{1u} + B_{3u}$, respectively. For the SC gap structure, the former has symmetry-protected point nodes on the k_y axes, whereas the latter has a line node on the $k_y = 0$ plane. Although it has not been settled which of the two representations corresponds to the LFSC or the HFSC states, the change in the SC gap structure would result in a change in the pinning force by modifying the interaction between vortices and impurities or defects. The anisotropy

of the SC gap influences both the vortex core and the lattice structure; the latter is discussed for the multiple SC states of UPt_3 [28,29].

Furthermore, if the IFSC state could be characterized by a mixing of the multiple SC components from the LFSC and HFSC states, i.e., $A_u^{\|b} + B_u^{\|b}$, then, as a consequence, the formation of nonsingular, coreless vortices may be expected [5,30–34]. Such coreless (fractional) vortices have been theoretically discussed, for example, in a field-induced chiral state of Sr_2RuO_2 [35], where the corresponding chiral state is characterized by degenerate pairing states with multiple (equal to four) components, and the fractional vortex lattice is suggested to be stabilized by the spin-orbit coupling. In general, vortices are pinned at impurities or defects, because the energy cost is minimized when the NC vortex cores are positioned at the impurities or defects, where the superconductivity is weaker or absent. In a nonsingular vortex state with multiple SC components, different components form vortex lattices separately, with the real-space positions of vortex cores shifted relative to each other [35,36]. This results in there being a nonzero SC order parameter everywhere, reducing the pinning force. In this case, several possibilities would explain the observed pinning around $B = 18$ T. One possibility is a matching between the lattice constants of the two vortex lattices, which may have different field dependencies. Another possibility is a first-order vortex-lattice phase transition, unique in such a mixed SC state. At magnetic fields just above (below) the LFSC-IFSC (IFSC-HFSC) transition field, the vortex lattice structure in the IFSC state would be mainly determined by the dominating LFSC (HFSC) order parameter. Then, there may be a phase transition between the two competing vortex structures at magnetic fields in the middle of the IFSC state. If this transition is of first order, there would be domains and domain walls, causing additional vortex pinning. It should be noted, however, that the formation of a nonsingular vortex state in bulk superconductors is still under debate. It has been argued that such a vortex state would be energetically unstable [33,37]. Since there are only few examples of superconductors with multiple SC states, further studies are needed to understand the vortex dynamics across different SC states in spin-triplet superconductors.

V. CONCLUSIONS

In conclusion, we studied the vortex dynamics in UTe_2 by measuring dc electrical resistivity with different currents along the a axis under magnetic fields along the b axis. We found a region of low critical current deep inside the SC state, which agrees with the recently proposed IFSC state [18]. The island formation of the low-critical-current region leads to an unusual maximum of critical current as a function of temperature. The accompanying decrease in the critical current with decreasing temperature cannot be explained by thermal fluctuations but is ascribed to the weakening of the pinning force. We discuss the possible origins for the weakening of the pinning force, including changes in the SC gap structure and nonsingular vortex states, which may host Majorana fermions [4,5]. Further intensive studies are required to understand the anomalous vortex state in spin-triplet superconductors.

ACKNOWLEDGMENTS

We thank J. Goryo, Y. Matsuda, M. Garst, T. Takimoto, Y. Nagai, and M. Machida for stimulating discussions. We thank M. Nagai and K. Shirasaki for experimental support. The work was supported by JSPS KAKENHI Grants No. JP20K20905, No. 20KK0061, No. JP21H05470, No. JP22H01176, No. JP22H00109, No. JP21K18145, No. JP22H04933, No. JP22H01181, and No. JP23K17353. This work (a part of the high-magnetic-field experiments) was performed at HFLSM under the IMR-GIMRT program (Proposals No. 202012-HMKPB-0012, No. 202112-HMKPB-0010, No. 202112-RDKGE-0036, and No. 202012-RDKGE-0084).

[1] G. Blatter, M. V. Feigel'man, V. B. Geshkenbein, A. I. Larkin, and V. M. Vinokur, Vortices in high-temperature superconductors, Rev. Mod. Phys. **66**, 1125 (1994).

[2] R. Okazaki, Y. Kasahara, H. Shishido, M. Konczykowski, K. Behnia, Y. Haga, T. D. Matsuda, Y. Onuki, T. Shibauchi, and Y. Matsuda, Flux line lattice melting and the formation of a coherent quasiparticle bloch state in the ultraclean URu_2Si_2 superconductor, Phys. Rev. Lett. **100**, 037004 (2008).

[3] B. Wu, D. Aoki, and J.-P. Brison, Vortex liquid phase in the p-wave ferromagnetic superconductor UCoGe, Phys. Rev. B **98**, 024517 (2018).

[4] N. Read and D. Green, Paired states of fermions in two dimensions with breaking of parity and time-reversal symmetries and the fractional quantum Hall effect, Phys. Rev. B **61**, 10267 (2000).

[5] D. A. Ivanov, Non-Abelian statistics of half-quantum vortices in p-wave superconductors, Phys. Rev. Lett. **86**, 268 (2001).

[6] S. Ran, C. Eckberg, Q.-P. Ding, Y. Furukawa, T. Metz, S. R. Saha, I.-L. Liu, M. Zic, H. Kim, J. Paglione, and N. P. Butch, Nearly ferromagnetic spin-triplet superconductivity, Science **365**, 684 (2019).

[7] D. Aoki, A. Nakamura, F. Honda, D. Li, Y. Homma, Y. Shimizu, Y. J. Sato, G. Knebel, J.-P. Brison, A. Pourret, D. Braithwaite, G. Lapertot, Q. Niu, M. Vališka, H. Harima, and J. Flouquet, Unconventional superconductivity in heavy fermion UTe_2, J. Phys. Soc. Jpn. **88**, 043702 (2019).

[8] G. Knebel, W. Knafo, A. Pourret, Q. Niu, M. Vališka, D. Braithwaite, G. Lapertot, M. Nardone, A. Zitouni, S. Mishra, I. Sheikin, G. Seyfarth, J.-P. Brison, D. Aoki, and J. Flouquet, Field-reentrant superconductivity close to a metamagnetic transition in the heavy-fermion superconductor UTe_2, J. Phys. Soc. Jpn. **88**, 063707 (2019).

[9] D. Aoki, F. Honda, G. Knebel, D. Braithwaite, A. Nakamura, D. Li, Y. Homma, Y. Shimizu, Y. J. Sato, J.-P. Brison, and

J. Flouquet, Multiple superconducting phases and unusual enhancement of the upper critical field in UTe_2, J. Phys. Soc. Jpn. **89**, 053705 (2020).

[10] K. Kinjo, H. Fujibayashi, S. Kitagawa, K. Ishida, Y. Tokunaga, H. Sakai, S. Kambe, A. Nakamura, Y. Shimizu, Y. Homma, D. X. Li, F. Honda, D. Aoki, K. Hiraki, M. Kimata, and T. Sasaki, Change of superconducting character in UTe_2 induced by magnetic field, Phys. Rev. B **107**, L060502 (2023).

[11] D. Aoki, J.-P. Brison, J. Flouquet, K. Ishida, G. Knebel, Y. Tokunaga, and Y. Yanase, Unconventional superconductivity in UTe_2, J. Phys.: Condens. Matter **34**, 243002 (2022).

[12] A. Rosuel, C. Marcenat, G. Knebel, T. Klein, A. Pourret, N. Marquardt, Q. Niu, S. Rousseau, A. Demuer, G. Seyfarth, G. Lapertot, D. Aoki, D. Braithwaite, J. Flouquet, and J. P. Brison, Field-induced tuning of the pairing state in a superconductor, Phys. Rev. X **13**, 011022 (2023).

[13] H. Fujibayashi, G. Nakamine, K. Kinjo, S. Kitagawa, K. Ishida, Y. Tokunaga, H. Sakai, S. Kambe, A. Nakamura, Y. Shimizu, Y. Homma, D. Li, F. Honda, and D. Aoki, Superconducting order parameter in UTe_2 determined by Knight shift measurement, J. Phys. Soc. Jpn. **91**, 043705 (2022).

[14] D. Braithwaite, M. Vališka, G. Knebel, G. Lapertot, J. P. Brison, A. Pourret, M. E. Zhitomirsky, J. Flouquet, F. Honda, and D. Aoki, Multiple superconducting phases in a nearly ferromagnetic system, Commun. Phys. **2**, 147 (2019).

[15] W.-C. Lin, D. J. Campbell, S. Ran, I.-L. Liu, H. Kim, A. H. Nevidomskyy, D. Graf, N. P. Butch, and J. Paglione, Tuning magnetic confinement of spin-triplet superconductivity, npj Quantum Mater. **5**, 68 (2020).

[16] L. Jiao, S. Howard, S. Ran, Z. Wang, J. O. Rodriguez, M. Sigrist, Z. Wang, N. P. Butch, and V. Madhavan, Chiral superconductivity in heavy-fermion metal UTe_2, Nature (London) **579**, 523 (2020).

[17] S. Kittaka, Y. Shimizu, T. Sakakibara, A. Nakamura, D. Li, Y. Homma, F. Honda, D. Aoki, and K. Machida, Orientation of point nodes and nonunitary triplet pairing tuned by the easy-axis magnetization in UTe_2, Phys. Rev. Res. **2**, 032014(R) (2020).

[18] H. Sakai, Y. Tokiwa, P. Opletal, M. Kimata, S. Awaji, T. Sasaki, D. Aoki, S. Kambe, Y. Tokunaga, and Y. Haga, Field induced multiple superconducting phases in UTe_2 along hard magnetic axis, Phys. Rev. Lett. **130**, 196002 (2023).

[19] Y. Haga, P. Opletal, Y. Tokiwa, E. Yamamoto, Y. Tokunaga, S. Kambe, and H. Sakai, Effect of uranium deficiency on normal and superconducting properties in unconventional superconductor UTe_2, J. Phys.: Condens. Matter **34**, 175601 (2022).

[20] P. F. S. Rosa, A. Weiland, S. S. Fender, B. L. Scott, F. Ronning, J. D. Thompson, E. D. Bauer, and S. M. Thomas, Single thermodynamic transition at 2 K in superconducting UTe_2 single crystals, Commun. Mater. **3**, 33 (2022).

[21] H. Sakai, P. Opletal, Y. Tokiwa, E. Yamamoto, Y. Tokunaga, S. Kambe, and Y. Haga, Single crystal growth of superconducting UTe_2 by molten salt flux method, Phys. Rev. Mater. **6**, 073401 (2022).

[22] D. Aoki, H. Sakai, P. Opletal, Y. Tokiwa, J. Ishizuka, Y. Yanase, H. Harima, A. Nakamura, D. Li, Y. Homma, Y. Shimizu, G. Knebel, J. Flouquet, and Y. Haga, First observation of the de Haas–van Alphen effect and Fermi surfaces in the unconventional superconductor UTe_2, J. Phys. Soc. Jpn. **91**, 083704 (2022).

[23] A. G. Eaton, T. I. Weinberger, N. J. M. Popiel, Z. Wu, A. J. Hickey, A. Cabala, J. Pospisil, J. Prokleska, T. Haidamak, G. Bastien, P. Opletal, H. Sakai, Y. Haga, R. Nowell, S. M. Benjamin, V. Sechovsky, G. G. Lonzarich, F. M. Grosche, and M. Valiska, Quasi-2D Fermi surface in the anomalous superconductor UTe_2, arXiv:2302.04758 [cond-mat.supr-con].

[24] C. Broyles, Z. Rehfuss, H. Siddiquee, J. A. Zhu, K. Zheng, M. Nikolo, D. Graf, J. Singleton, and S. Ran, Revealing a 3d Fermi surface pocket and electron-hole tunneling in UTe_2 with quantum oscillations, Phys. Rev. Lett. **131**, 036501 (2023).

[25] D. Aoki, I. Sheikin, A. McCollam, J. Ishizuka, Y. Yanase, G. Lapertot, J. Flouquet, and G. Knebel, de Haas–van Alphen oscillations for the field along c-axis in UTe_2, J. Phys. Soc. Jpn. **92**, 065002 (2023).

[26] Y. Tokiwa, P. Opletal, H. Sakai, K. Kubo, E. Yamamoto, S. Kambe, M. Kimata, S. Awaji, T. Sasaki, D. Aoki, Y. Tokunaga, and Y. Haga, Stabilization of superconductivity by metamagnetism in an easy-axis magnetic field on UTe_2, arXiv:2210.11769 [cond-mat.supr-con].

[27] J. Ishizuka, S. Sumita, A. Daido, and Y. Yanase, Insulator-metal transition and topological superconductivity in UTe_2 from a first-principles calculation, Phys. Rev. Lett. **123**, 217001 (2019).

[28] M. Ichioka, A. Hasegawa, and K. Machida, Field dependence of the vortex structure in d-wave and s-wave superconductors, Phys. Rev. B **59**, 8902 (1999).

[29] A. Huxley, P. Rodière, D. M. Paul, N. van Dijk, R. Cubitt, and J. Flouquet, Realignment of the flux-line lattice by a change in the symmetry of superconductivity in UPt_3, Nature (London) **406**, 160 (2000).

[30] N. D. Mermin and T.-L. Ho, Circulation and angular momentum in the A phase of superfluid helium-3, Phys. Rev. Lett. **36**, 594 (1976); **36**, 832(E) (1976).

[31] P. W. Anderson and G. Toulouse, Phase slippage without vortex cores: Vortex textures in superfluid ^{3}He, Phys. Rev. Lett. **38**, 508 (1977).

[32] M. M. Salomaa and G. E. Volovik, Quantized vortices in superfluid ^{3}He, Rev. Mod. Phys. **59**, 533 (1987).

[33] M. Sigrist and K. Ueda, Phenomenological theory of unconventional superconductivity, Rev. Mod. Phys. **63**, 239 (1991).

[34] S. Autti, V. V. Dmitriev, J. T. Mäkinen, A. A. Soldatov, G. E. Volovik, A. N. Yudin, V. V. Zavjalov, and V. B. Eltsov, Observation of half-quantum vortices in topological superfluid ^{3}He, Phys. Rev. Lett. **117**, 255301 (2016).

[35] S. Takamatsu and Y. Yanase, Spin-triplet pairing state of Sr_2RuO_4 in the c-axis magnetic field, J. Phys. Soc. Jpn. **82**, 063706 (2013).

[36] S. B. Chung, D. F. Agterberg, and E.-A. Kim, Fractional vortex lattice structures in spin-triplet superconductors, New J. Phys. **11**, 085004 (2009).

[37] E. Babaev, Vortices with fractional flux in two-gap superconductors and in extended faddeev model, Phys. Rev. Lett. **89**, 067001 (2002).